Available online at www.sciencedirect.com
SCIENCE DIRECT®
Journal of Molecular Catalysis A: Chemical 215 (2004) 95–101
JOURNAL OF MOLECULAR CATALYSIS A: CHEMICAL
www.elsevier.com/locate/molcata

Active phases of supported cobalt catalysts for 2,3-dihydrofuran synthesis

Ludmila Leite[a,*], Vladislavs Stonkus[a], Kristine Edolfa[a], Luba Ilieva[b], Donka Andreeva[b], Ludmila Plyasova[c], Janusz W. Sobczak[d], Sorana Ionescu[e], Gabriel Munteanu[e]

[a] *Latvian Institute of Organic Synthesis, 21 Aizkraukles Str., Riga LV-1006, Latvia*
[b] *Institute of Catalysis, Bulgarian Academy of Sciences, 1113 Sofija, Bulgaria*
[c] *Boreskov Institute of Catalysis, Russian Academy of Sciences Siberian Division, 5 Acad. Lavrentjev Str., Novosibirsk, 630090, Russia*
[d] *Institute of Physical Chemistry, Polish Academy of Sciences, Kasprzaka 44/52 Str., 01-224 Warszawa, Poland*
[e] *Romanian Academy Institute of Physical Chemistry "I.G. Murgulescu", 202 Splaiul Independentei St., 77208-Bucharest, Romania*

Received 24 October 2003; accepted 11 November 2003

Abstract

Dehydrogenation of 1,4-butanediol to 2,3-dihydrofuran over kaolin-supported Co and Co–Au catalysts has been investigated. Catalytic test and XRD analysis show that the presence of metallic cobalt with hexagonal structure is favourable for selectivity to 2,3-dihydrofuran of the reaction studied. It was established by XPS method that an optimal for the reaction selectivity Co^0/Co^{2+} ratio in Co/kaolin and Co–Au/kaolin catalysts exists. Quantum chemical calculations suggest that the initial step of 1,4-butanediol dehydrogenation on cobalt catalyst surface may be the cleavage of O–H bond to form alkoxide species on Co^{2+} ion. Based on the effect of metallic and ionic cobalt on the catalyst selectivity, it could be presumed that both cobalt species are involved in the rate-determining step in dehydrogenation of 1,4-butanediol into 4-hydroxybutanal intermediate.

Keywords: Cobalt catalyst; Gold promotion; 1,4-Butanediol; 2,3-Dihydrofuran; Dehydrogenation

1. Introduction

Dehydrogenation of alcohols gives commodity chemicals of a considerable industrial use, on which many studies are focused. Dehydrogenation of methanol, ethanol, propanol, 2-propanol, octanol, and cyclohexanol proceeds mainly in the presence of metal oxides having basic properties [1–4] and metallic or bimetallic catalysts [5,6].

The role of cobalt either in metallic or in ionic state is not yet clear, and the nature of the active sites in dehydrogenation reactions is still debated. Now more and more data indicate that ionic species may play an important role in dehydrogenation. On the other hand, it was established that in the case of cyclohexanol dehydrogenation on metallic cobalt catalyst, the incomplete reduction of the metal oxide favours the cyclohexene formation (side reaction) by direct cyclohexanol dehydration [6].

The conversion of 1,4-butanediol on supported cobalt, copper and platinum catalysts has been studied [7–11]. The reaction occurs through several sequence reactions (such as shown in Scheme 1) leading to the formation of 2,3-dihydrofuran and tetrahydrofuran.

This scheme includes 1,4-butanediol dehydrogenation into 4-hydroxybutanal. Our experimental data suggests that dehydrogenation is a rate-limited stage in the synthesis of 2,3-dihydrofuran [8]. Almost quantitative 2,3-dihydrofuran formation is a result of the subsequent fast isomerization of 4-hydroxybutanal and dehydration of 2-hydroxytetrahydrofuran over the support.

Recently, we established that the modification of supported cobalt catalyst by gold is favourable for 2,3-dehydrofuran synthesis, concerning not only the enhanced catalyst reducibility, which is desirable in order to lower the pretreatment temperature, but also the catalyst selectivity [7,12].

The aim of the present study is to throw light on the active phases regarding a possible participation of cobalt in metallic and ionic states in 1,4-butanediol transformation to 2,3-dihydrofuran, over cobalt/kaolin catalysts, being non-promoted and promoted by gold.

* Corresponding author. Tel.: +371-7551822; fax: +371-7821038.
E-mail address: leite@osi.lv (L. Leite).

1381-1169/$ – see front matter © 2004 Elsevier B.V. All rights reserved.
doi:10.1016/j.molcata.2003.11.036

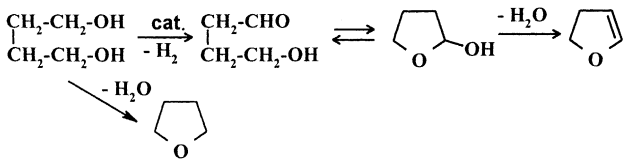

Scheme 1.

2. Experimental

2.1. Materials

1,4-Butanediol used was a commercial product with a purity of at least 97%. Kaolin purchased from "Acros" and air-calcined at 750 °C for 5 h, with BET surface area of 22.7 m^2/g and average particle size of 570 nm was used as a support. Cobalt loading was 40%. The amount of Au in gold-containing samples was equal to 4 wt.%, corresponding to an atomic Co/Au ratio of 1/0.04.

The catalysts were prepared as follows: cobalt or gold–cobalt-containing precursors were prepared by precipitation of $Co(NO_3)_2{\cdot}6H_2O$, respectively, co-precipitation of $HAuCl_4{\cdot}3H_2O$ and $Co(NO_3)_2{\cdot}6H_2O$ with a sodium carbonate solution. Precipitation was carried out in an automated laboratory reactor "Contalab" ("Contraves" Switzerland), under a complete control of all the parameters of preparation. The precipitate was filtered and carefully washed. The samples were dried at 120 °C. All the substances used were of an analytical grade. A mechanical mixture between the precursors and the support was made in the next step of the catalysts preparation. Catalyst samples were activated by reduction in a hydrogen stream for 20 min at different temperatures chosen concerning the TPR data obtained recently [12]. After reduction, the sample was cooled to an ambient temperature in a N_2 stream and placed quickly into the reactor with 1,4-butanediol and under a constant nitrogen feed, i.e. under conditions securing the absence of the contact with O_2.

3. Methods

XPS measurements were performed using VG Scientific ESCALAB-210 spectrometer. An Al Kα radiation source operated at a power of 300 W (15 kV, 20 mA) was applied. Vacuum in the analysis chamber was below 6×10^{-9} mbar during all measurements. Pass energy of 20 eV and step of 0.1 eV was used. The spectrometer binding energy scale was calibrated by the Ag $3d_{5/2}$ peak at 368.27 eV and Ag M_4NN peak at 895.75 eV. The data obtained were analysed using ECLIPSE VG program, including satellite subtraction, Shirley shape background subtraction and fitting procedure. Quantification was made by MULTILINE program [13]. Binding energies for cobalt species were determined with respect to silicon in kaoline support, BE Si 2 s at 154.00 eV [14]. Samples were pressed in the form of pellets, mounted on heated sample holder and introduced inside the XPS spectrometer. Any grinding procedure was used before pressing the pellets. The Co 2p, Au 4f, Al 2p, Si 2p, Si 2s, O 1s, C 1s and the valence band energy regions were recorded before and after hydrogen reduction at different temperatures and intervals. Reduction was performed in situ in the preparation chamber using 6.0 hydrogen. The identification of surface cobalt species was made according to [14–18].

The XRD study was performed on a diffractometer URD-6 (Germany). Cu–Kα radiation and graphite monochromator on the diffraction beam were used. The diffraction patterns were recorded by 0.05° step scanning at a 2θ angle range from 10 to 70° and the accumulation period of 30 s at each point. The XRD data were used to determine the catalysts phase composition and particle size. The c.s.d. (coherent scattering domain) of metallic particles was determined by the Sherrer method [19] using the half-width of the diffraction reflections: for Au (1 1 1) [20]; for Co (1 1 1) or (2 0 0) cubic structure [21] and for Co(1 0 1) hexagonal structure [22].

The calculations were performed with a Linux PC version of the GAMESS [23] package at the HF level, using the TZV wave functions as basis set. The cobalt in a ionic state was modelled as a Co^{2+} ion placed within a distance of a few angstroms from the reactant molecule. Full optimisation of the reactants and products as well as transition state (TS) location were performed. The TS was characterized by calculating the hessian, and performing intrinsic reaction co-ordinate calculations (IRC).

The catalytic activity test was performed as described previously [12], in a glass reactor equipped with a dropping funnel, a stirrer, a thermometer, and a port for nitrogen introduction. The catalyst to feed-stock weight ratio was *ca* 1:43. The products formed in the reaction of 1,4-butanediol were distilled off and collected in a water-cooled condenser and dry-ice cooled vapour trap. They were analysed by means of gas-chromatography. The reaction was conducted in N_2 at atmospheric pressure in a 200–240 °C temperature range.

2,3-Dihydrofuran (2,3-DHF), tetrahydrofuran (THF) and unidentified resinous substances (NP) were the main products detected in the reaction mixture. During the reaction studied, the conversion of 1,4-butanediol (1,4-BD) was usually 100% (the yield is equal to the selectivity in this case) except of the reaction in the presence of catalyst containing Co^{cub}.

The yield and selectivity were calculated in following way:

$$\text{yield (mol\%)} = \frac{\text{g of 2, 3-DHF formed} \times \text{molar weight of 1, 4-BD} \times 100}{\text{g of 1, 4-BD taken in feed} \times \text{molar weight of 2, 3-DHF}}$$

selectivity (%)

$$= \frac{\text{g of 2, 3-DHF formed} \times \text{molar weight of 1, 4-BD}}{\text{g of 1, 4-BD converted} \times \text{molar weight of 2, 3-DHF}} \times 100$$

The mass balance was >95%.

4. Results and discussion

The data on the yield of 2,3-DHF in the reaction of 1,4-BD over Co/kaolin and Co–Au/kaolin catalysts after reduction pre-treatment at different temperature are presented in Fig. 1.

The chosen temperatures for the reduction of gold-promoted catalyst are lower than those of the non-promoted one due to the enhanced catalysts reduction in the presence of gold in accordance with the TPR results obtained [7,12]. In both cases of non-promoted and promoted supported cobalt catalysts, the reducibility of cobalt is limited. The fact that some cobalt species remain in an unreducible state is known from the literature and it has been explained concerning the small particle size and a strong support interaction [18,24].

The modification by gold is favourable concerning not only the reduction temperature but also the catalyst selectivity. The selectivity depends significantly on the reduction temperature, and Fig. 1 clearly demonstrates a maximum of the yield of 2,3-dihydrofuran both in the presence of the non-promoted and promoted by gold–cobalt catalysts. The optimum temperature depends on the cobalt loading [25] and modification. For 40% Co/kaolin it is equal to 470 °C and for 35% Co–5% Au/kaolin – to 330 °C, respectively. The yield of 2,3-DHF on Co–Au/kaolin catalyst reduced at 330 °C, is higher than that of non-promoted catalyst reduced at 470 °C. Even when the pre-treatment reduction temperature of the Au–Co/kaolin sample is lower than the optimal one, the yield of 2,3-DHF is approximately the same as of the non-promoted catalyst (see the yield after reduction at 300 and 470 °C, respectively).

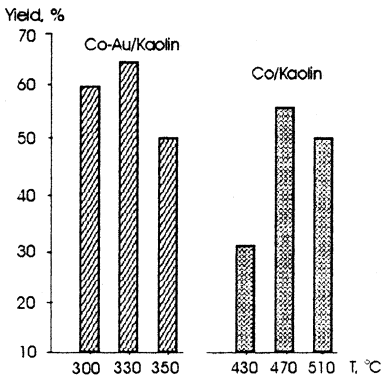

Fig. 1. Dependence of the 2,3-dihydrofuran yield on the catalyst reduction temperature.

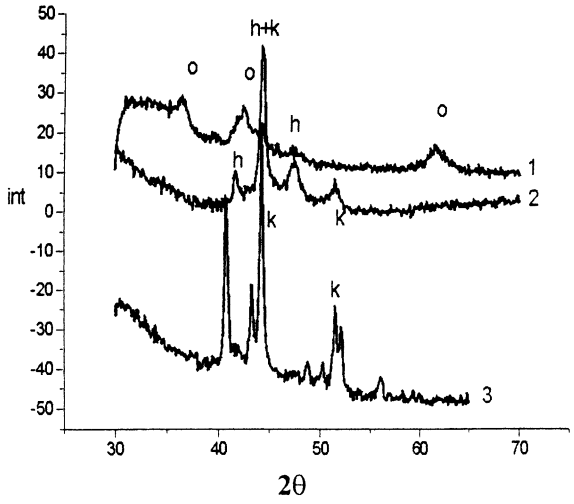

Fig. 2. XRD-patterns of Co/kaolin samples after reduction at 340 (1), 470 (2), and 650 °C (3). Designations: **k** and **h**-cobalt of cubic or hexagonal structure, respectively; **o**: CoO; without designations: aluminosilicate.

It was established by XRD analysis that the reduction of Co/kaolin studied occurs via CoO formation (Fig. 2, curve 1). After the treatment of the catalyst sample in H_2 at 470 °C, a reduction to metallic cobalt phase with hexagonal (Co^{hex}) and cubic (Co^{cub}) structure takes place (Fig. 2, curve 2). The increase of the reduction temperature up to 650 °C leads to the enlargement of the Co^{cub} particles size up to 400 Å, while the average particles size of hexagonal Co structure decreases to approximately 50 Å (Fig. 2, curve 3).

In the XRD pattern of Co–Au/kaolin sample reduced at 340 °C (Fig. 3, curve 1), there are lines of a nanosize phase ($\delta = 60$ Å) of metallic cobalt with hexagonal structure [22] and gold with an average particle size of approximately 250 Å [20]. It is seen in the diffractogram (Fig. 3, curve 2) that after the reduction of Co–Au/kaolin sample at 650 °C,

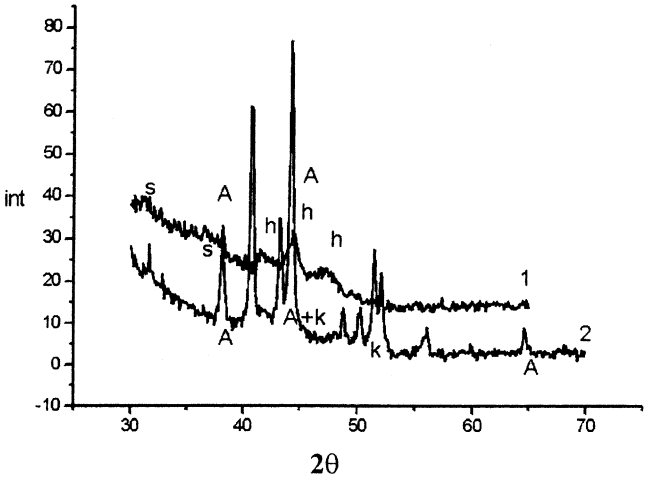

Fig. 3. XRD-patterns of Co–Au/kaolin (D) after reduction at 340 °C (1) and at 650 °C (2). Designations: **k** and **h**–cobalt of cubic or hexagonal structure; **A**: gold; **S**: trace of CoAlSiO-compound; without designations—aluminosilicate.

Table 1
Catalytic properties of metallic cobalt: different phases of cobalt-kaolin catalysts in the conversion of 1,4-butanediol

Catalyst	Catalyst reduction temperature (°C)	Phase	Yield (%)			Specific activity in relation to 2,3-DHF formation ($g \times g_{cat}^{-1} \times h^{-1}$)
			2,3-DHF	THF	NP	
Co–Au/kaolin	300	Co^{hex}	60	10	27	3.8
Co–Au/kaolin	330	Co^{hex}	66	11	21	4.3
Co/kaolin	470	$Co^{hex} + Co^{cub}$	57	11	29	3.7
Co–Au/kaolin[a]	650	Co^{cub}	20	10	50	1.3

[a] Conversion of 1,4-BD is 82%, selectivity to 2,3-DHF 30%.

the amount of metallic Co sharply grows and the particles sinter up to the size of 450 Å. The Co structure is cubic with the lattice parameter $a = 3.5447$ Å [21].

The different state of the metallic cobalt phases after reduction at various temperatures (340, 470, and 650 °C) is in agreement with the literature data [19]. According to these data, the equilibrium state of cobalt at temperatures below 450 °C is a Co^{hex}, and at temperature higher than 450 °C it is a Co^{cub}. Near to the phase transition point a metastable biphases state, corresponding to the microdomains of both structures, can be observed [26]. Due to the enhanced reducibility in the presence of gold, the reduction of cobalt to metallic state occurs at a temperature <450 °C. That is why only Co^{hex} is present in the case of Co–Au catalyst after reduction at 340 °C.

Taking into account the XRD results and the higher activity of gold-promoted catalyst in relation to 2,3-DHF formation than that of non-promoted one (Fig. 1), it may be suggested that the selectivity of the reaction studied is connected with the structure of the metallic cobalt phase. A comparison of the 2,3-DHF yield and specific activity of Co/kaolin and Co–Au/kaolin catalysts shows that Co^{hex} is more favourable for 2,3-DHF formation than Co^{cub} (Table 1).

A low value of the specific activity of Co–Au sample reduced at 650 °C and containing only Co^{cub} may be due to the lower activity of such form of cobalt, as well as may be connected with the growth of particle size up to 450 Å. Recently, it has been also established that the cubic cobalt is less active than hexagonal cobalt in the Fischer–Tropsch synthesis [27].

To explain the interesting experimental fact, i.e. the presence of the maxima in the yield of 2,3-DHF which depends on the reduction temperature of both Co and Co–Au catalysts (Fig. 1), XPS analysis was applied for the study of a corresponding oxidation state of surface cobalt. Due to relatively small shifts, absolute value of binding energy of $2p_{3/2}$ peak is not very useful for distinguish between Co^{+3} and Co^{+2} oxides. However, presence of secondary features of the spectra as satellite structures, arising from interaction of emitted photoelectrons with core vacancy is a characteristic for Co^{2+} only, not for Co^{3+} and Co^{0}. Such structures at approximately 787 eV are visible in both catalysts in unreduced state in Figs. 4(a) and 5(a). Together with peaks at 781.3 eV, this exhibit presence of Co^{2+} in unreduced samples. After reduction, the main peak of Co $2p_{3/2}$, diminishes to values of BE to about 777.8 eV, which is a characteristic to supported metallic cobalt [17,18].

Detailed decomposition of the spectra shows that the reduction is not complete as part of Co^{+2} species still is visible on the surface. The ratio of the peak area of the metallic component to the total area of Co $2p_{3/2}$ peak can be used as a measure for the extent of reduction (Table 2). Due to complexity of Co 2p spectra, this method is not very accurate. However, obtained extent of reduction is in good agreement with values obtained for Co/SiO_2 by Reuel and Bartholomew [28] or Niemelä et al. [29]. It is worth to

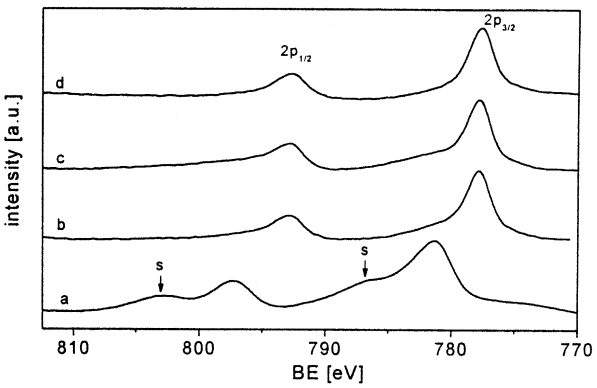

Fig. 4. XPS spectra in the Co 2p region of Co/kaolin reduced at different temperatures: (a) unreduced state; (b), (c), (d) samples reduced at 450, 470 and 490 °C, respectively.

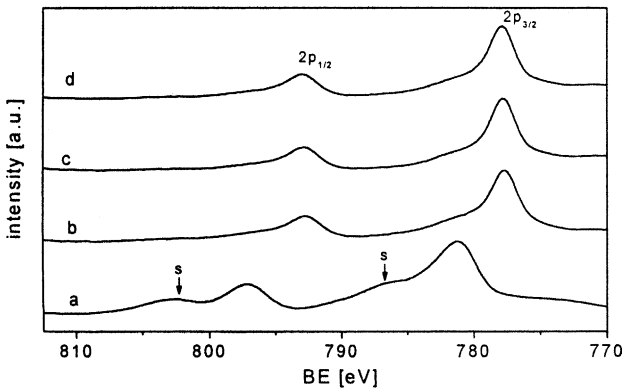

Fig. 5. XPS spectra in the Co 2p region of Co–Au/kaolin reduced at different temperatures (a) unreduced state; (b), (c), (d) samples reduced at 310, 330 and 350 °C, respectively.

Table 2
XPS data of Co/kaolin (Co) and Co–Au/kaolin (Co–Au) catalysts

Sample	Reduction (T, °C)	Concentration (at.%)		Co^0/Co^{2+} ratio	BE		
		Co^0	Co^{2+}		Co^{2+} sat.	Co^{2+}	CO^0
Co	before reduction	0	100		785.35	781.34	
Co	450	76.72	23.28	3.3	782.83	780.25	777.87
Co	470	81.73	18.27	4.5	782.76	780.43	777.89
Co	490	83.09	16.91	4.9	782.54	780.08	777.75
Co–Au	before reduction	0	100		785.83	781.32	
Co–Au	310	75.76	24.25	3.1	783.01	780.51	777.69
Co–Au	330	77.26	22.74	3.4	782.97	780.60	777.84
Co–Au	350	80.42	19.58	4.1	782.72	780.36	777.89

underline that for Co–Au/kaoline reduction, to this extent, was obtained in much lower temperatures.

Full reduction of cobalt to metal form probably can be impossible due to encapsulation part of Co species by support (possible) and/or due to formation of non-reducible cobalt aluminosilicates.

Direct comparison of the Co 2p spectra for both series of catalyst show that catalysts Co–Au/kaolin have visible broadening of Co $2p_{3/2}$ peak (Fig. 6). This may indicate a higher Co dispersion in Co–Au/kaolin. Intensity of Au 4f peaks increase after first and sequenced reduction stages (Fig. 7). Value of BE Au $4f_{7/2}$ changes from 84.35 eV before reduction to 83.4 eV after reduction. Similar value of negative shift of BE was observed for palladium–gold alloys [14].

Thus, the correlation between the catalytic results and the reduction degree of surface cobalt shows that when the presence of metallic cobalt of Co/kaolin catalyst is higher than approximately 82%, the yield of 2,3-dihydrofuran decreases. In the case of Co–Au/kaolin, the optimal Co^0 content is approximately 77%. It may mean that an optimum ratio of metallic cobalt/cobalt in ionic state exists for the reaction studied.

The influence of the reduction extent on Co/Al_2O_3 catalyst activity in the Fischer–Tropsch reaction was noted by Schanke et al., however in this case, the active phase is metallic cobalt and its oxidation causes the catalyst deactivation [30].

The mechanism of alcohol dehydrogenation on metal and metal oxides has been investigated by many scientists [31–36]. As a chemical intermediate, the surface alkoxide formation was suggested in most cases. Some authors have been studying IR and EPR spectra of methanol, ethanol, and propanol—adsorbed on Co and Cu supported catalysts [31–33]. It was suggested that the initial step in the dehydrogenation reaction is the formation of alkoxide species on Co^{2+} and Cu^{2+} and its further transformation to aldehyde or ketone. It has been confirmed that the abstraction of an α-hydrogen from methanol results in the formation of the corresponding aldehyde, is the rate-determing step in the dehydrogenation process [36].

The mechanism of ethanol dehydrogenation was also studied by quantum chemical methods. Two possible dehydrogenation mechanisms of ethanol over metal oxide via surface ethoxy groups generation have been proposed. Concerning the first mechanism, the surface metal ion and oxygen ion concertedly interact with oxygen and hydrogen of the OH group, respectively. An H_α of the ethoxy group then shifts to a surface proton resulting in acetaldehyde and a molecular hydrogen formation. According to the second mechanism, a proton of OH group and α-proton of ethanol

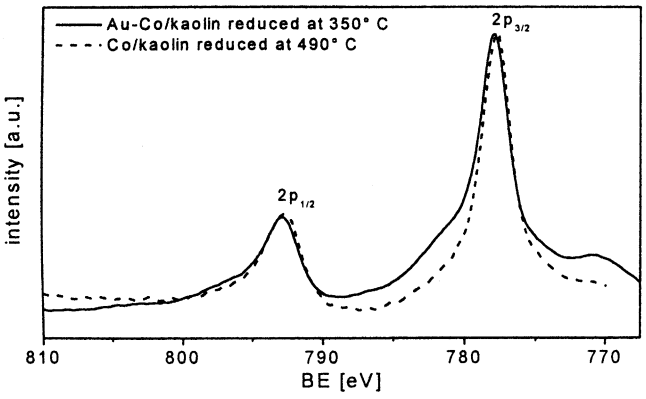

Fig. 6. Example of comparison Co 2p in Au–Co/kaolin and Co/kaolin (reduced at highest temperatures).

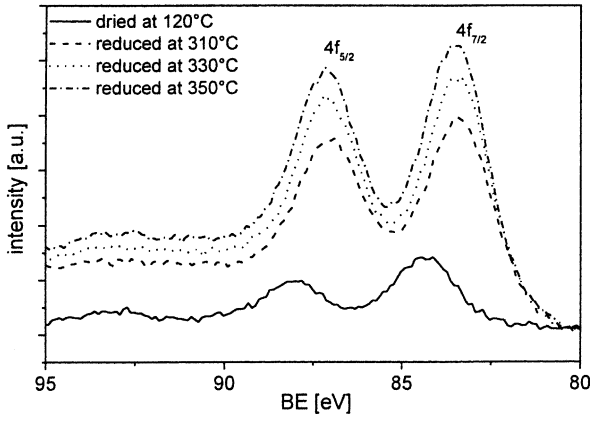

Fig. 7. XPS spectra in the Au 4f region of Co–Au/kaolin reduced at different temperatures.

Table 3
Bond orders of the main molecular bonds characteristic to the compounds involved in the dehydrogenation reaction of 1,4-butanediol both in the presence of Co^{2+} and in its absence

Bond	Bond order					
	1,4-Butanediol (optimised geometry)		1,4-Butanediol (transition state)		Aldehyde + hydrogen(optimised geometry)	
	Without Co^{2+}	With Co^{2+}	Without Co^{2+}	With Co^{2+}	Without Co^{2+}	With Co^{2+}
O–H (1)	0.824	0.711	0.633	0.085	–	–
C–H (1)	0.953	0.922	0.526	0.641	–	–
O–C (1)	0.818	0.450	1.229	0.398	1.902	1.166
H–H (1)	0.000	0.000	0.248	0.294	1.000	1.000
O–H (2)	0.824	0.790	0.817	0.795	0.822	0.790
C–H (2)	0.953	0.827	0.948	0.937	0.952	0.939
O–C (2)	0.818	1.417	0.840	0.873	0.821	0.869

are extracted simultaneously by the surface oxygen and metal ions [37,38]. The mechanism of other alkanol dehydrogenation reactions has received relatively less attention in literature.

A marked effect of cobalt cation quantity on the 1,4-BD conversion to 2,3-DHF could indicate that cobalt in the ionic state participates in the rate-determining step, i.e. in 1,4-BD dehydrogenation, to form 4-hydroxybutanal. In the presence of kaolin-supported Co catalysts, dehydrogenation and dehydration of 1,4-BD occurs. That is why we considered the necessity to clarify the influence of Co^{2+} ion on C–OH, O–H and C_α–H bonds by ab initio quantum chemical calculations. The results obtained are presented in Table 3. The reacting bonds of 1,4-butanediol molecule are noted as (1), while the other similar bonds are noted as (2).

In order to explain the necessity of cobalt cation presence in the active catalyst, the bond orders (BO) analysis was performed. BO is a measure of the bond strength and can be useful in monitoring the reaction mechanism [37,38].

On the basis of BO analysis, it was found that in the presence of Co^{2+} the bonds O–H and C_α–H (breaking in the 1,4-BD dehydrogenation) are weaker (smaller BO) than in the isolated molecule and in this way they are activated for 4-hydroxybutanal formation. The BO of C–O bond also decreases in the presence of Co^{2+}, meaning that the dehydration process is also possible. Nevertheless, the TS located indicates that the O–H and C_α–H BO decreases, whereas the C–O BO increases, reaching a value close to that for a double bond in the products (aldehyde formation). At the same time it can be seen that the single bond in the hydrogen molecule is formed.

The second O–H, C–O and C_α–H bonds in the 1,4-BD molecule have unchanged BO and they are not weakened by the presence of Co^{2+} ion, meaning that a further dehydrogenation of 4-hydroxybutanal is highly improbable.

The catalytic effect of Co^{2+} results in decreasing the activation energy from 175 kcal/mol (in the absence of the Co^{2+} ion) down to 103 kcal/mol (in its presence). The activation energy was calculated as the difference between the total energy of the optimised reactant and of the TS.

Another effect consists of the modification of the reaction mechanism. As it can be seen in Table 3, in the absence of the catalyst the C_α–H bond breaks first, whereas in the presence of Co^{2+} the hydroxylic H shifts first and the O–H bond is practically broken at the TS point. In fact, the literature data indicate that the dehydrogenation of alcohols on metal oxides takes place with formation of an alkoxide species adsorbed on the surface.

The alkanols can also adsorb on metallic species [34,39] but it has been established that the degree of adsorption decreases in the presence of hydrogen.

On the basis of our experimental and theoretical studies as well as on the literature data on catalytic dehydrogenation of alcohols, it can be proposed that both metallic and ionic cobalt take part in the dehydrogenation reaction stage. Most probably the first step of the reaction studied is a dissociative adsorption of 1,4-BD molecule on an active site consisting of a pair of metal-oxygen ions and the formation of an alkoxide species. It is also possible that in our case the alkoxide species are formed on metal cobalt as it is shown by IR method in relation to the surface 2-propoxide intermediate formation on Ni^0 [34]. The fact that the catalyst reduction to a high metal cobalt content is an essential stage of catalyst pre-treatment may mean that the metallic cobalt takes part in the rate-determined stage of proton abstraction from C_α atom of 1,4-BD molecule. After cleavage of the organometallic bond formed between cobalt and oxygen atom of diol, alkoxide intermediate migrates to the kaolin support and it undergoes isomerization and dehydration to form 2,3-DHF. Hydrogen atoms are removed probably by migration to Co^0 sites, recombination, and desorption as H_2. The interaction of ionic and metallic sites via migration of hydrogen atoms formed in C_α–H and O–H bond of alkanol to metal was suggested by Iglesia et al. [40]. It was suggested that Co^0 and Co^{2+} sites are located within a molecular distance so that migration and adsorption of H atoms are possible. The necessity of bicentric active phase formed by metallic cobalt in interaction with CoO was assumed by Enache et al. for cobalt-based Fischer–Tropsch catalyst [27]. The cooperative behaviour of Co^{2+} and Co^0 surface sites is an essential requirement for the 1,4-BD

dehydrogenation to 4-hydroxybutanal, studied in the present paper.

5. Conclusions

- Our catalytic results and XRD analysis have shown that the yield of 2,3-dihydrofuran is sensitive to the dispersion of catalyst particle and the metallic Co form (Co^{hex} or Co^{cub}). The presence of Co^{hex} is favourable for the yield 2,3-dihydrofuran in the reaction studied.
- Dehydrogenation catalytic properties of the supported cobalt catalysts in the 1,4-butanediol transformation to 2,3-dihydrofuran depend on a certain ratio between the surface quantity of cobalt in metallic and ionic states. By means of XPS, it was established that the values of the optimal Co^0/Co^{2+} ratios of Co/kaolin and Co–Au/kaolin catalyst reduced at the optimal temperatures (470 and 330 °C, respectively) are close.
- Based on the effect of metallic and ionic cobalt on the catalyst selectivity, it could be suggested that both cobalt species are involved in the rate-determing step in dehydrogenation of 1,4-butanediol into 4-hydroxybutanal intermediate.
- Quantum chemical calculations suggest that the initial step of the 1,4-butanediol dehydrogenation on cobalt catalyst surface may be the cleavage of O–H bond to form alkoxide species on Co^{2+} ion.

Acknowledgements

We thank Dr. T. Tabakova for the catalysts synthesis.

References

[1] P. Sabatier, A. Mailhe, Ann. de Chem. et de Phys. 20 (1910) 289.
[2] S.A. Halawy, M.A. Mohamed, S.F. Abd El-Hafez, J. Mol. Catal. A: Chemical 94 (1994) 191.
[3] D.V. Cesar, C.A. Peréz, V.M. Salim, M. Schinal, Appl. Catal. A Ceneral 176 (1999) 205.
[4] S. Chokkaram, R. Srinivasan, D.R. Milburn, B.H. Davis, J. Mol. Catal. A: Chemical 121 (1997) 157.
[5] R. Barth, J.S. Falcone Jr., Sh. Vorce, J. McLennan, B. Outland, E. Amoth, Cat. Commun. 33 (2002) 135.
[6] H. Idriss, E.G. Seebauer, J. Mol. Catal. A: Chemical 152 (2000) 201.
[7] L. Leite, V. Stonkus, L. Ilieva, D. Andreeva, T. Tabakova, Bulg. Chem. Comm. 33 (2001) 148.
[8] L. Leite, A. Lebedev, V. Stonkus, M. Fleisher, J. Mol. Catal. A: Chemical 144 (1999) 323.
[9] P. Dimroth, H. Pasedach, Angew. Chem. 72 (1960) 865.
[10] M. Bartók, Á. Molnár, Acta Chim. Acad. Sci. Hung. 100 (1979) 203.
[11] I.I. Geiman, L.F. Bulenkova, A.A. Lazdinsh, A.K. Veinberg, V.A. Slavinskaya, A.A. Avots, Chem. Heterocycl. Compds. 4 (1981) 448.
[12] L. Leite, V. Stonkus, L. Ilieva, L. Plyasova, T. Tabakova, D. Andreeva, E. Lukevics, Catal. Commun. 3 (2002) 341.
[13] A. Jablonski, B. Lesiak, L. Zommer, M.F. Ebel, H. Ebel, Y. Fukuda, Y. Suzuki, S. Tougaard, Surf. Interface Anal. 21 (1994) 724.
[14] NIST XPS DataBase v.3 (http://srdata.nist.gov/xps).
[15] J.F. Moulder, W.F. Stickle, P.E. Sobol, K.D. Bomben, Handbook of X-ray Photoelectron Spectroscopy, Perkin-Elmer Corp., Physical Electronics Division, Eden Praire, Minnesota, 1992.
[16] A. Galtayries, J. Grimblot, J. Electr. Spectr. 98–99 (1999) 267.
[17] R. Riva, H. Miessner, R. Vitali, G. Del Piero, Appl. Catal. A. 196 (2000) 111.
[18] B. Ernst, A. Bensaddik, L. Hilaire, P. Chaumette, A. Kiennemann, Catal. Today 39 (1998) 329.
[19] A. Guinier, Theorie et Technigue de la Radiocrystallographie. Dunod, Paris, 1956, p. 458.
[20] X-ray PDF, JCPDS, card 05-0727.
[21] X-ray PDF, JCPDS, card 04-0784.
[22] X-ray PDF, JCPDS, card 15-0806.
[23] M.W. Schmidt, K.K. Baidridge, J.A. Boatz, S.T. Elbert, M.S. Gordon, J.H. Jensen, N.S. Koseki, N. Matsunaga, K.A. Nguyen, S.J. Su, T.L. Windus, M. Depuis, J.A. Montgomery, J. Comput. Chem. 14 (1993) 1347.
[24] L. Guczi, L. Borko, Z. Schay, D. Bazin, F. Mizukami, Catal. Today 65 (2001) 51.
[25] V. Stonkus, L. Leite, A. Lebedev, E. Lukevics, A. Ruplis, J. Stoch, M. Mikolajczyk, J. Chem. Technol. Biotechnol. 76 (2001) 101.
[26] A. Khassin, T. Yurieva, V. Zaikovckii, L. Plyasova, V. Parmon, Kinetika i kataliz 39 (1998) 431.
[27] D.I. Enache, B. Rebours, M. Roy-Auberger, R. Revel, J. Catal. 205 (2002) 346.
[28] R.C. Reuel, C.H. Bartholomew, J. Catal. 85 (1984) 63–78.
[29] M.K. Niemelä, L. Backnian, A.O.I. Krause, T. Vaara, Appl. Catal. A. 156 (1997) 319.
[30] D. Schanke, A. M Hilmen, E. Bergene, K. Kinnary, E. Ritter, E. Adnanes, A. Holmen, Catal. Lett. 34 (1995) 269.
[31] I.D. Miheikin, J.U.I. Pecherskaya, V.B. Kazanskii, Kinetika i kataliz 12 (1971) 191.
[32] G. Blyholder, D. Shihabi, in: Proceedings of the 6th International Congress on Catalysis, London, 1976, A34.
[33] J.E. Bailie, C.H. Rochester, G.J. Hutching, J. Chem. Soc. Faraday Trans. 93 (1997) 4389.
[34] L.J. Shorthouse, A.J. Roberts, R. Raval, Surf. Sci. 480 (2001) 37.
[35] H. Idriss, E.G. Seebauer, Catal. Lett. 66 (2000) 139.
[36] S. Göbölös, M. Hegedüs, I. Kolosova, M. Maciejewski, J.L. Margitfalvi, Appl. Catal. A: General 169 (1998) 201.
[37] Y. Shinohara, H. Satozono, T. Nakajima, S. Suzuki, S.H. Mishima, J. Chem. Software 4 (1997) 41.
[38] Y. Shinohara, T. Nakajima, S. Suzuki, S.H. Mishima, H. Ishikawa, J. Chem. Software 4 (1997) 89.
[39] G.D. Zakumbaeva, Interaction between Organic Compounds and Surface of VIII Group Metal, Nauka, 1978, p. 229.
[40] E. Iglesia, D.G. Barton, J.A. Biscardi, M.J.L. Gines, S.L. Soled, Catal. Today 38 (1997) 339.